STUDIA UBB CHEMIA, LXVIII, 2, 2023 (p. 23-36)
(RECOMMENDED CITATION)
DOI:10.24193/subbchem.2023.2.02

MYRICETIN AS CORROSION INHIBITOR FOR METALS IN ALCOHOLIC SOLUTIONS

Cristian George VASZILCSIN[a], Mihai V. PUTZ[a,b], Mircea L. DAN[c,*], Mihai MEDELEANU[c]

ABSTRACT. Corrosion inhibitory effect of myricetin in alcoholic solutions has been studied by potentiodynamic polarization. Inhibitory efficiencies of 70%, 61%, 69% and 79% have been obtained for stainless steel, carbon steel, aluminum alloy, and aluminum, respectively. Adsorption Gibbs free energy, determined using Langmuir adsorption isotherms, has revealed that interactions between metal atoms and myricetin adsorbed molecules have chemical character. Moreover, quantum chemistry calculations have shown that myricetin, due to its molecular structure (O heteroatoms with lone pair electrons and π electrons from aromatic rings) has the ability to form an adsorption layer on the metal surface that inhibits the diffusion of molecules and ions participating in the global corrosion process.

Keywords: *myricetin*, *corrosion inhibitor*, *potentiodynamic polarization*, *adsorption isotherm, food industry*.

[a] *National Institute of Research and Development in Electrochemistry and Condensed Matter, Dr. A. Paunescu Podeanu street 144, 300569 Timişoara, Romania*
[b] *Faculty of Chemistry, Biology, Geography, West University of Timişoara, Pestalozzi street 16A, 300115 Timisoara, Romania*
[c] *Faculty of Industrial Chemistry and Environmental Engineering, University Politehnica Timişoara, V. Pârvan Bd. 6, 300223 Timişoara, Romania*
* *Corresponding author: mircea.dan@upt.ro*

INTRODUCTION

Corrosion of metals and alloys can cause significant damages, especially by the shutdown of the industrial equipment or even entire plants. The total cost produced by corrosion in the US economic sectors (infrastructure, utilities, transportation, production and government) was about $137.9 billion per year [1]. As well, there are economic sectors, like the food and pharmaceutical industry, where corrosion can lead to the contamination of products with heavy metal ions, which can compromise their quality and make them unusable. In these circumstances, it is necessary to carefully select the most suitable materials, especially metals and alloys, used in the manufacturing of the equipment, pipelines or storage tanks [2,3].

The corrosion rate of metals and alloys depends both on their nature and aggressiveness of the environment in contact with the metal. It is well known that in the pharmaceutical and food industry, in various processes of dissolution, extraction or washing, aqueous solutions of ethyl alcohol are used, which are aggressive for a lot of metals and alloys [4].

Over the years, several methods have been developed to reduce the corrosion rate depending on the metal nature and environmental aggressiveness. One of the most applied anti-corrosion protection methods is the use of adsorption inhibitors. They are generally organic compounds, which at very low concentrations substantially decrease the corrosion rate. Their effect is due to the formation of a molecular layer of inhibitor adsorbed on the metal surface, which avoids the diffusion of chemical species participating in the corrosion process [5].

The current legislative regulations allow the use as inhibitors only of non-toxic organic compounds, which do not contaminate the environment. For this reason, researchers' attention has been focused on the use of natural products, friendly to the environment, known as "green inhibitors" [6,7]. They are usually compounds of natural origin, such as: proteins, amino acids, alkaloids, tannins, polyphenols, flavonoids and others [8-11].

According to the results presented in the literature, the corrosion of metals in contact with aqueous solutions is inhibited by organic compounds containing various structures like heteroatoms of O, N, S and/or P, having lone pair electrons, or π electrons belonging to aromatic rings or multiple bonds [12].

Among the flavonoid compounds having anti-corrosive potential myricetin (MYR) should be mentioned, with structural formula given in the Figure 1. The IUPAC name of MYR is 3,5,7-trihydroxy-2-(3,4,5-trihydroxyphenyl)-4-chromenone.

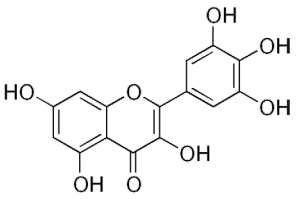

Figure 1. Structural formula of myricetin

MYR can be found in various plants from which it can be extracted using selective solvents [13,14]. Natural extracts containing MYR were tested as corrosion inhibitors for mild steel in 0.5 HCl [15], 0.5 M H_2SO_4 [16] and 3.5% NaCl [17] or for tin in 3% NaCl [18].

The aim of this paper is the study of the electrochemical behavior of MYR, as well as the inhibiting activity on the corrosion process of stainless steel W14301 (AISI 304), carbon steel (OLC 45), aluminum alloys (3004 ASTM) and pure aluminum in synthetic alcoholic solutions.

RESULTS AND DISCUSSION

Potentiodynamic polarization

The MYR effect on corrosion rate of the tested metals has been studied in alcoholic environment, in the absence and presences of different inhibitor concentration by potentiodynamic polarization (PDP) [19]. Polarization curves were drawn after immersing the metal in the test solution for 1 hour, enough time to establish an equilibrium or quasi-equilibrium at the metal – solution interface. Potentiodynamic curves recorded at 1 mV s^{-1} scan rate are shown in Figure 2a-d for all metals.

Potentiometric parameters evaluated from linear voltammograms as a function of MYR concentration are the following: corrosion current density (i_{corr}), corrosion potential (E_{corr}), anodic (b_a) and cathodic (b_c) Tafel slope and polarization resistance (R_p). The inhibition efficiency (IE) and surface coverage (θ) have been calculated using relationships (1) and (2). The polarization resistance has been evaluated using Stern-Geary relationship.

The obtained values are presented in Table 1 for stainless steel and carbon steel and Table 2 for aluminum alloy and aluminum.

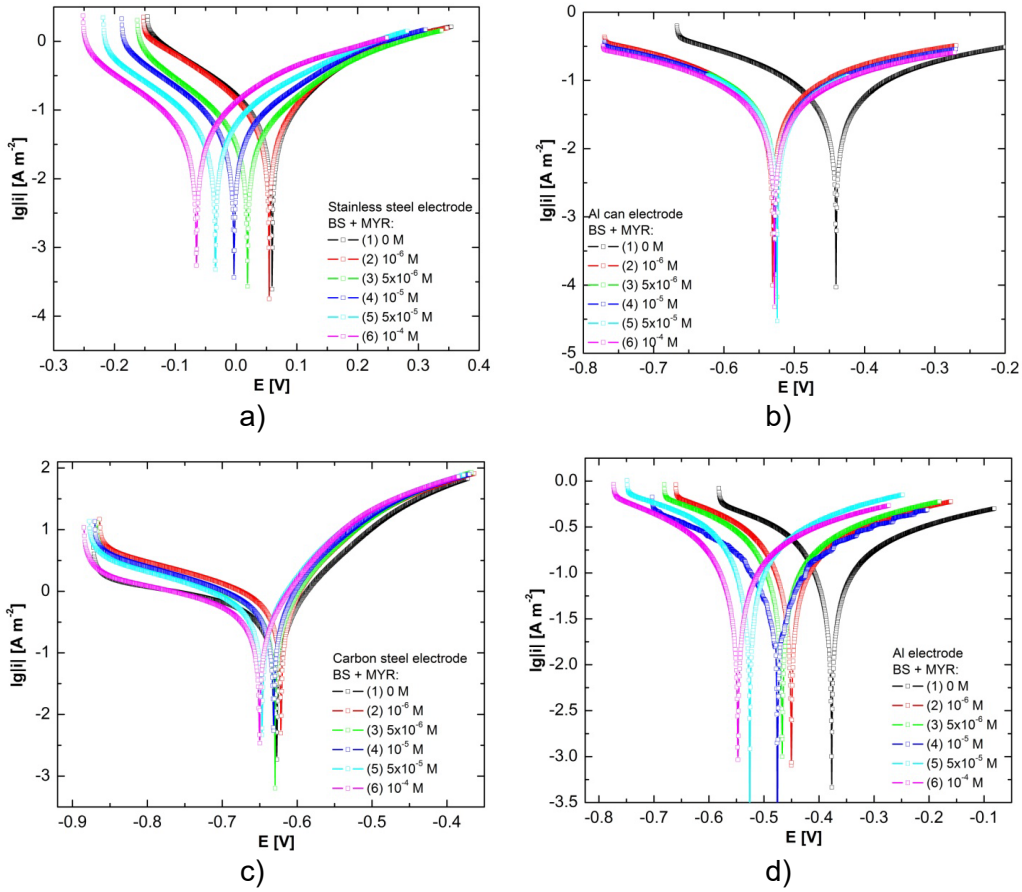

Figure 2. Linear voltammograms recorded on 304L (a), Al alloy (b), carbon steel (c) and Al (d) in test solutions at 25°C, scan rate 1 mV s^{-1}.

The results obtained by PDP show that the presence of MYR in the alcoholic solution has a significant anticorrosive effect, even at low concentrations. Thus, at a concentration of 10^{-4} M, which means about 30 ppm, the inhibitory efficiency was 70% (304L), 61% (carbon steel), 69% (Al alloy) and 79% (Al).

It should be emphasized that MYR is stable in the base solution. As it follows from the CVs, MYR does not undergo electrochemical reactions even when the working electrode is polarized in the anodic or cathodic direction.

Table 1. Polarization parameters for the corrosion of stainless steel and carbon steel in test solutions

Metal	Inh. conc. [M]	i_{corr} [μA cm^{-2}]	E_{corr} [mV]	$-b_c$ [mV]	b_a [mV]	R_p [Ω]	*IE* [%]	θ
304L	0 (BS)	6.78	-59.1	163	173	4053	-	-
	10^{-6}	6.02	-52.5	167	164	4233	11.2	0.11
	$5\cdot10^{-6}$	4.97	-15.4	171	149	5488	26.7	0.27
	10^{-5}	4.12	6.71	175	147	6053	39.2	0.39
	$5\cdot10^{-5}$	3.23	38.6	178	141	6450	52.4	0.52
	10^{-4}	2.01	67.2	182	140	6917	70.4	0.70
OLC 45	0 (BS)	69.37	-627	95.2	327	273	-	-
	10^{-6}	62.28	-623	93.3	287	306	10.2	0.10
	$5\cdot10^{-6}$	53.05	-631	90.4	289	353	23.5	0.24
	10^{-5}	44.04	-633	88.4	268	392	36.5	0.37
	$5\cdot10^{-5}$	37.42	-646	83.8	261	442	46.1	0.46
	10^{-4}	26.77	-651	77.5	258	521	61.4	0.61

Table 2. Polarization parameters for the corrosion of aluminum alloy and aluminum in test solutions

Metal	c_{inh} [M]	i_{corr} [μA cm^{-2}]	E_{corr} [mV]	$-b_c$ [mV]	b_a [mV]	$R_p\cdot10^{-3}$ [Ω]	*IE* [%]	θ
Al alloy	0 (BS)	6.73	-440	331	289	8.7	-	-
	10^{-6}	5.05	-514	314	288	9.3	25.0	0.25
	$5\cdot10^{-6}$	4.46	-520	303	281	10	33.7	0.34
	10^{-5}	4.01	-524	280	272	12.4	40.4	0.40
	$5\cdot10^{-5}$	3.62	-528	265	253	14.6	46.2	0.46
	10^{-4}	2.11	-534	256	243	17.7	68.7	0.69
Al	0 (BS)	43.5	-374	428	279	2.29	-	-
	10^{-6}	33.73	-451	436	300	2.64	22.5	0.22
	$5\cdot10^{-6}$	26.18	-467	443	322	3.07	39.8	0.40
	10^{-5}	19.9	-481	452	351	3.59	54.2	0.54
	$5\cdot10^{-5}$	14.1	-512	458	368	4.09	67.6	0.68
	10^{-4}	8.95	-545	471	379	4.69	79.4	0.79

Adsorption isotherms

The results obtained by PDP were fitted using the Langmuir, Freundlich, Frumkin, Temkin, Flory-Huggins and El-Awady adsorption isotherms, the best fit being obtained for the Langmuir isotherm, linearized in the form of equation (3), for which the correlation coefficients r^2 were 0.989 (304L), 0.990 (OLC 45), 0.973 (Al alloy) and 0.998 (Al).

Knowing the adsorption constant, the values of the adsorption Gibbs free energy ΔG^o_{ads} were calculated, according to relation (4).

The adsorption Gibbs free energy gives information on the nature of the interaction between the metal and the inhibitor molecules in the adsorption layer.

The adsorption Gibbs free energy gives information on the interaction nature between the metal and the inhibitor molecules in the adsorption layer. It is known that if ΔG^o_{ads} > –20 kJ mol^{-1}, then the adsorption has a physical character, and if ΔG^o_{ads} < –40 kJ mol^{-1}, then chemical bonds are involved in the adsorption process of inhibitor molecules on the metal. The above conditions are known as the "20/40 rule" [20].

Figure 3 shows the Langmuir isotherms for the four studied metals. From the ordinate, the adsorption constant K_{ads} is calculated, then the adsorption Gibbs free energy ΔG^o_{ads} is obtained using relationship (4). The results are listed in Table 3.

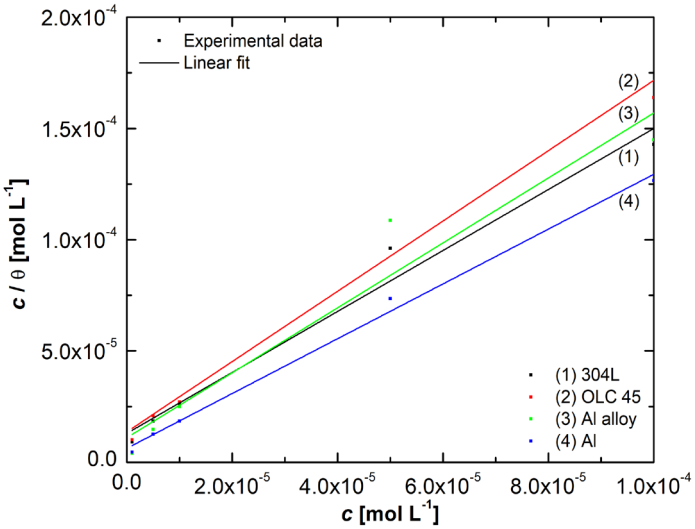

Figure 3. Langmuir isotherms for 304L (1), OLC 45 (2), Al alloy (3) and Al (4)

Table 3. Langmuir parameters

Metal	Intercept	r^2	K_{ads}	ΔG^o_{ads} [kJ mol^{-1}]
304L	1.296·10^{-5}	0.989	77160	-37.8
OLC 45	1.365·10^{-5}	0.990	73260	-37.7
Al alloy	1.101·10^{-5}	0.973	90827	-38.2
Al	6.246·10^{-6}	0.998	160102	-39.6

The values obtained for ΔG_{ads}^{o} show that interactions between the metal atoms and adsorbed MYR molecules have a chemical character and, consequently, high values of the inhibitory efficiency are expected.

Quanto-chemical evaluation of the inhibitory effect of myricetin

The "20/40 rule" is par excellence empirical and does not uniquely characterize the inhibitory efficiency of an organic compound, so that the evaluation of the molecular parameters of the inhibitors is useful as well.

The molecular parameters for MYR were determined by DFT (density functional theory) using B3LYP functional and the 6-311G(dp) basis set calculations using Gaussian software [21]. In order to compare the molecular parameters of MYR with those of other organic compounds, calculations were performed for quercetin (QUE), trans-resveratrol (TRV) and capsaicin (CPS). The fitted primary data are given in Table 4.

Table 4. DFT primary data for MYR

Compound	Dipole moment [D]	E_{HOMO} [eV]	E_{LUMO} [eV]	ΔE
MYR	7.059	-5.521	-1.765	3.756
QUE	6.417	-5.517	-1.778	3.739
TRV	2.617	-5.481	-1.488	3.993
CPS	3.261	-5.698	-0.139	5.559

There is no simple dependency relationship between the inhibitory effect of the organic compound and its molecular characteristics. In general, an appreciable dipole moment preferentially orients the molecules at the metal - solution interface, but this orientation is favorable only if it provides as large a coverage surface as possible. On the other hand, the orientation determined by the dipole moment can be annihilated by chemical interactions between the metal and the π electrons or lone pairs electrons of the oxygen atoms from the inhibitor molecule. The dipole moment value of MYR (7.059 D) is appreciable compared to other natural compounds, such as TRV (2.617 D), CPS (3.261 D) and QUE (6.417 D). However, since the metal-inhibitor interaction has chemical nature, as it results from the adsorption Gibbs free energy ΔG_{ads}^{o}, determined based on the Langmuir adsorption isotherm, the influence of the dipole moment on the conformation of the MYR molecule on the metal surface is insignificant.

Unlike the dipole moment, the molecular parameters E_{HOMO}, E_{LUMO} and $\Delta E = E_{LUMO} - E_{HOMO}$ have a significant influence on the inhibitory properties. Figure 4 shows the values of these parameters for MYR and the other three natural compounds, taken as terms of comparison. On the one hand, higher values for E_{HOMO} increase the ability of the inhibitor to share electrons with the metal, on the other hand, lower values of E_{LUMO} increase the ability to accept electrons from the metal. Therefore, the smaller the difference ΔE, the higher the probability of forming metal-inhibitor chemical interactions.

It can be seen that for TRV, MYR and QUE the E_{HOMO} energy is approximately the same. For MYR and QUE, the same values were obtained for E_{LUMO}, which means that, for the two compounds, the ΔE differences are approximately equal. From this point of view, no great differences are expected between the inhibitory efficiencies of MYR and QUE, under the same conditions, since their structural formulas are very similar. For TRV, E_{LUMO}, is lower and ΔE higher than for MYR and QUE, therefore, it is probable to obtain a lower inhibitory efficiency for TRV than MYR and QUE, respectively. For CPS, the E_{HOMO} value is the lowest, therefore the ability to donate electrons to the metal is the lowest, while the E_{LUMO} value is the highest, which decreases the ability to accept electrons from the metal. It is expected that under the same conditions, the inhibitory efficiency of CPS is the lowest among the four organic compounds.

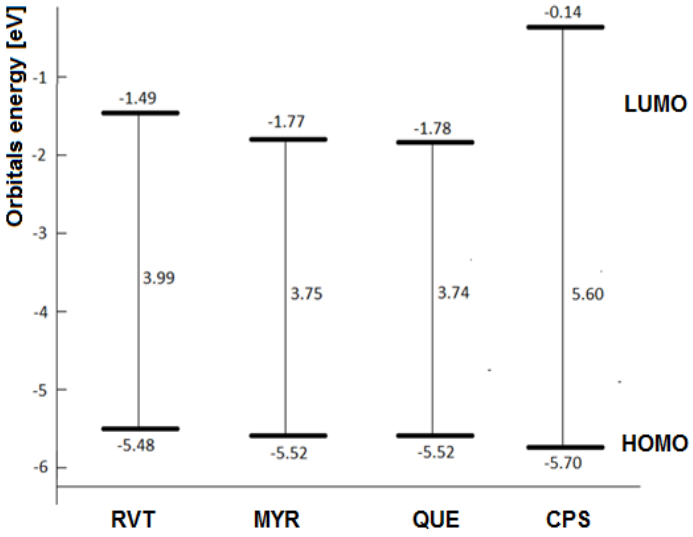

Figure 4. The values of molecular parameters E_{HOMO}, E_{LUMO} and ΔE

These assessments have a certain degree of uncertainty, since the three parameters E_{HOMO}, E_{LUMO} and ΔE are not sufficient to evaluate the inhibitory capacity.

Compared to other natural compounds, MYR has higher E_{HOMO} values. For example, the following E_{HOMO} values were reported for α-pinene, limonene, α-terpineol, p-cymene and p-cymen-8-ol: -6.07; -6.30; -6.30; -6.39; -6.33 eV. At the same time, the values for E_{LUMO} are generally higher: +0.37; +0.24; +0.44; +0.18; -0.19 eV [22]. Under these conditions, the probability to obtain higher inhibitory efficiencies for MYR compared to the above natural compounds is very high.

Recently, results close to those obtained for MYR have been reported. Zehra et al. evaluated the molecular parameters for the natural products catechin, vitexin-4'-O-glucoside-2''-O-hamnoside, vitexin-4'-O-rhamnoside, quercetin-3-glucoside and chlorogenic acid. For E_{HOMO} the values of -5.5202 -5.9149; -5.8855; -5.4571, respectively -5.8320 eV have been obtained, while for E_{LUMO}, the values were: -1.575; -1.4402; -1.4196; -1.5417, respectively -1.7827 eV. In 1 M HCl solutions, for carbon steel, the efficiencies reported for these inhibitors had values up to 94% [23]. Certainly, the inhibitory efficiencies are not directly comparable, since they do not refer to the same metal and the same corrosive environment.

An image of the possibilities to achieve some chemical interactions is given by the HOMO and LUMO distribution in the inhibitor molecule (Figure 5), drawn using Chemcraft - graphical software for visualization of quantum chemistry computations [24].

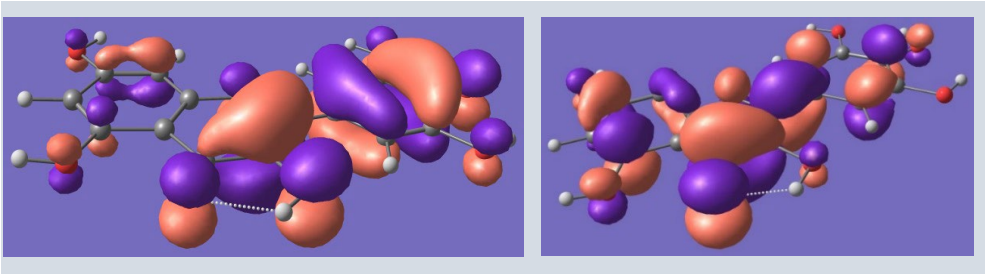

Figure 5. Distribution of HOMO and LUMO orbitals in MYR molecule.

The maximum density of HOMO orbitals in the MYR molecule is distributed over the isolated aromatic ring, while the maximum density of LUMO orbitals is found on the two condensed rings (an aromatic ring and a heterocycle with oxygen). As a result, the interactions of the inhibitor

molecules with the metal have chemical nature in which both the isolated aromatic cycle and the two condensed cycles participate. Considering the molecular structure, MYR can adopt plane-parallel conformations to the metal surface, thus ensuring a maximum coverage area. Even if the molecular dipole moment is large, the plane-parallel conformation to the metal surface of the inhibitor molecules will not be disturbed significantly due to the fact that the interaction between the molecular dipole and the electric field at the metal-solution interface is much weaker than chemical interactions. As a result, the MYR molecule is expected to possess good inhibitory properties.

EXPERIMENTAL SECTION

Materials and methods

Electrochemical tests were performed in a 100 mL corrosion glass cell consisted of the studied metal specimen having 0.8 cm^2 exposed area as working electrode, two graphite counter electrodes, and a Ag/AgCl electrode as reference. All potentials were referred versus the reference electrode ($E_{Ag/AgCl}$ = +0.197 V/NHE). Experiments were performed in 12% ethanol + 0.25 M Na_2SO_4 solution in which MYR concentrations was between 10^{-6} and 10^{-4} M. The role of Na_2SO_4 is to increase the electrolyte solution conductivity for a better data accuracy.

Sodium sulphate ≥99.0% (Fluka™) and Ethylic alcohol 95% - Spectrogravimetric grade Sigma-Aldrich) have been used to prepare the test solutions.

Electrochemical studies were carried out using a BioLogic SP150 potentiostat galvanostat. Before each experiment the test solutions were deaerated by bubbling high purity nitrogen. The working electrode (stainless steel, carbon steel, aluminum alloy and aluminum) was abraded with different grit emery papers, cleaned in ultrasonic bath, washed with distilled water and finally dried. The electrode potential was allowed to stabilize 60 min before starting the measurements. The inhibitory effect was studied by potentiodynamic polarization, providing information about the inhibitory efficiency.

The inhibitory efficiency was calculated from voltammetric data, using the corrosion current densities (1) [25].

$$\eta_{inh} = \frac{i_{cor(o)} - i_{cor(inh)}}{i_{cor(o)}} \cdot 100\ \% \quad (1)$$

where $i_{cor(o)}$ is the corrosion current density in the absence of the inhibitor, A m^{-2}, $i_{cor(inh)}$ - corrosion current density in the presence of the inhibitor, A m^{-2}.

Surface coverage of the metal by the inhibitor molecules is given by the relationship (2) [26].

$$\theta = \frac{\eta_{inh}}{100} \quad (2)$$

Adsorption isotherms Langmuir, Freundlich, Frumkin, Temkin, Flory-Huggins and El-Awady have been used in order to evaluate adsorption constant K_{ads}, respectively adsorption Gibbs free energy ΔG^o_{ads}. The best the fit has been obtained by Langmuir isotherm, given in a linear form in Eq. 3 [27].

$$\frac{c_{inh}}{\theta} = \frac{1}{K_{ads}} + c_{inh} \quad (3)$$

where c_{inh} is the concentration of the inhibitor, mol L^{-1}; θ - surface coverage; K_{ads} - adsorption constant.

Knowing the adsorption constant K_{ads}, the standard value of the adsorption Gibbs free energy ΔG^o_{ads} can be calculated, according to the relation (4) [27].

$$\Delta G^o_{ads} = -RTln(c_{H_2O(aq)} \cdot K_{ads}) = -RTln(55.5 \cdot K_{ads}) \quad (4)$$

where R is the universal gas constant (8.314 J mol^{-1} K^{-1}; T - thermodynamic temperature, K; $c_{H_2O(aq)}$ - concentration of water in the electrolyte solution.

For highly diluted solutions, the molar concentration of water is 55.5 mol L^{-1}.

The molecular parameters were determined using the Gaussean software [21].

The elemental composition of the steels is given in Table 5 - for OLC 45 and table 6 - for AISI 304L, and for pure aluminum - in Table 7. For the studied aluminum alloy, the elemental composition is given in Table 8.

Table 5. Elemental composition of the carbon steel OLC 45

Elm.	Fe	C	Si	Mn	P	S	Cr	Ni
% wt	96.98	0.4184	0.2510	0.7920	0.0132	0.0335	1.162	0.029
Elm.	Mo	Cu	Al	Ti	V	Co	Nb	W
% wt	0.2123	0.0234	0.0229	<0.004	0.0124	0.0222	<0.001	<0.010

Table 6. Elemental composition of the stainless steel 304L

Elm.	Fe	C	Si	Mn	P	S	Cr	Ni
% wt	64.89	0.030	1.000	2.00	0.05	0.030	20.0	12.0

Table 7. Elemental composition of pure aluminum

Elm.	Al	Fe	Si	Mn	Cu	Mg	Zn	Ti
[%] wt	99.67	0.21	0.03	0.01	0.03	0.01	0.02	0.01

Table 8. Elemental composition of aluminum alloy

Elm.	Al	Fe	Si	Mn	Cu	Mg	Zn	Ti	Others
[%] wt	95.58	0.69	0.29	1.42	0.24	1.18	0.22	0.24	0.14

CONCLUSIONS

The myricetin molecule contains structural elements that allow strong chemical bonds with metal atoms, which gives it anticorrosive properties for carbon steel, stainless steel, aluminum and aluminum alloys. The values of the Gibbs free energy of adsorptionΔG^{o}_{ads},, determined based on Langmuir isotherms, confirmed that the interactions between the studied metals and myricetin molecules are chemical, close to -40 kJ mol^{-1}.

Quanto-chemical calculations performed on the basis of Gaussian software revealed that the molecular parameters of myricetin allow strong adsorption at the interface metal - electrolyte solution, with beneficial effects on the anticorrosive properties.

The corrosion rates and inhibitory efficiency of myricetin was studied in alcoholic solutions for 304L stainless steel, OLC 45 carbon steel, aluminum and 3004 ASTM aluminum alloy, using the potentiodynamic polarization method. Even at very low concentrations, 10^{-4} mol L^{-1}, which means approximately 30 ppm, myricetin has an appreciable inhibitory efficiency: 70% (304L), 61% (OLC 45), 69% (Al alloy) and 79 % (Al). For stainless steel and aluminum alloy, the corrosion current densities in the presence of myricetin (10^{-4} mol L^{-1}) are about 2 μA cm^{-2}, while for pure aluminum it is almost 10 μA cm^{-2}, and in the case of carbon steel it exceeds 25 μA cm^{-2}. Certainly, these low values do not affect the mechanical and physical qualities of the studied metals, but the use of carbon steel and pure aluminum in the food and pharmaceutical industry must be done with caution to avoid contamination of processed products with metal ions.

ACKNOWLEDGMENTS

This work was carried out with the partial support of the West University of Timisoara, as well as the University Politehnica Timisoara. As well, the authors are grateful for the support from the National Institute for Research and Development in Electrochemistry and Condensed Matter from Timisoara.

REFERENCES

1. P. R. Roberge; *Corrosion Engineering*, McGraw Hill, New York, **2008**, 14-17.
2. A. Zaffora; F. Di Franco; M. Santamaria; *Curr. Opin. Electrochem.*, **2021**, *29*, 100760.
3. V. Alar; B. Runje; F. Ivušić; A. Horvatić; M. Mihaljević; *Metalurgija,* **2016**, *55*, 437-440.
4. M. Santamaria; G. Tranchida; F. Di Franco; *Corros. Sci.*, **2020**, *173*, 108778.
5. G. Sh. Jassim; A. M. B. Al-Dhalimy; A. S. Noori; M. H. Shadhar; M. M. Kadhim; H. A. Almashhadani; A. M. Rheima; P. Liu; *Inorg Chem Comun.*, **2022**, *142*, 109650.
6. A. I. Ikeuba; O. B. John; V. M. Bassey; H. Louis; A. U. Agobi; J. E. Ntibi; F. C. Asogwa; *Results Chem.*, **2022**, *4*, 100543.
7. S. Z. Salleh; A. H. Yusoff; S. K. Zakaria; M. A. A. Taib; A. A. Seman; M. N. Masri; M. Mohamad; S. Mamat; S. A. Sobri; A. Ali; P. T. Teo; *J. Clean Prod.*, **2021**, *304*, 127030.
8. B. El Ibrahimi; A. Jmiai; L. Bazzi; S. El Issami; *Arab. J. Chem.*, **2020**, *13*, 740-771.
9. N. Chaubey; Savita; A. Quraishi; D. S. Chauhan; M. A. Quraishi; *J. Mol. Liq.*, **2021**, *321*, 114385.
10. K. W. Tan; M. J. Kassim; C. W. Oo; *Corros. Sci.*, **2012**, *65*, 152-162.
11. S. Varvara; G. Caniglia; J. Izquierdo; R. Bostan; L. Găină; O. Bobis; R. M. Souto; *Corros. Sci.*, **2020**, *165*, 108381.
12. J. N. Pejic; B. V. Jegdic; B. M. Radojkovic; D. D. Marunkic; A. D. Marinkovic; J. B. Bajat; *Corros. Sci.*, **2022**, *209*, 110815.
13. S. H. Alrefaee; K. Y. Rhee; C. Verma; M. A. Quraishi; E. E. Ebenso; *J. Mol. Liq.*, **2021**, *321*, 114666.
14. S. Donkor; Z. Song; L. Jiang; H. Chu; *J. Mol. Liq.*, **2022**, *359*, 119260.
15. A. Thakur; A. Kumar; S. Sharma; R. Ganjoo; H. Assad; *Mater. Today - Proceedings,* **2022**, *66*, 609-621.
16. R. Haldhar; D. Prasad; A. Saxena; R. Kumar; *Sustain. Chem. Pharm.*, **2018***, 9*, 95-105.
17. S. A. Haddadi; E. Alibakhshi; G. Bahlakeh; B. Ramezanzadeh; M. Mahdavian; *J. Mol. Liq.*, **2019**, *284*, 682-699.
18. I. Radojcic; K. Berkovic; S. Kovac; J. Vorkapic-Furac; *Corros. Sci.*, **2008**, *50*, 1498-1504.
19. O. Demidenko; A. M. Popescu; K. Yanushkevich; E. I. Neacsu; C. Donath; V. Constantin; *Studia UBB Chemia,* **2022**, *LXVII, 2*, 67-77.
20. A. Kokalj, 2021. Corrosion inhibitors: physisorbed or chemisorbed?, *Corros. Sci.*, **2021**, *196*, 109939.
21. *Gaussian 09*, Revision B.01, M. J. Frisch, G. W. Trucks, H. B. Schlegel, G. E. Scuseria, M. A. Robb, J. R. Cheeseman, G. Scalmani, V. Barone, B. Mennucci, G. A. Petersson, H. Nakatsuji, M. Caricato, X. Li, H. P. Hratchian, A. F. Izmaylov, J. Bloino, G. Zheng, J. L. Sonnenberg, M. Hada, M. Ehara, K. Toyota, R. Fukuda, J. Hasegawa, M. Ishida, T. Nakajima, Y. Honda, O. Kitao, H. Nakai,

T. Vreven, J. A. Montgomery, Jr., J. E. Peralta, F. Ogliaro, M. Bearpark, J. J. Heyd, E. Brothers, K. N. Kudin, V. N. Staroverov, T. Keith, R. Kobayashi, J. Normand, K. Raghavachari, A. Rendell, J. C. Burant, S. S. Iyengar, J. Tomasi, M. Cossi, N. Rega, J. M. Millam, M. Klene, J. E. Knox, J. B. Cross, V. Bakken, C. Adamo, J. Jaramillo, R. Gomperts, R. E. Stratmann, O. Yazyev, A. J. Austin, R. Cammi, C. Pomelli, J. W. Ochterski, R. L. Martin, K. Morokuma, V. G. Zakrzewski, G. A. Voth, P. Salvador, J. J. Dannenberg, S. Dapprich, A. D. Daniels, O. Farkas, J. B. Foresman, J. V. Ortiz, J. Cioslowski, and D. J. Fox, Gaussian, Inc., Wallingford CT, **2010**.

22. M. Barbouchi; B. Benzidia; A. Aouidate; A. Ghaleb; M. El Idrissi; M. Choukrad; *J. King. Saud. Univ. Sci.*, **2020**, *32*, 2995-3004.
23. B. F. Zehra; A. Said; H. M. Eddine; E. Hamid; H. Najat; N. Rachid; L. Toumert; *J. Mol. Struct.*, **2022**, *1259*, 132737.
24. https://www.chemcraftprog.com (accessed 06.12.2022)
25. A. F. Szőke; C. Filiâtre; L. M. Mureșan; *Studia UBB Chemia,* **2022**, *LXVII, 2*, 175-191.
26. M. Bobina; A. Kellenberger; J. P. Millet; C. Muntean; N. Vaszilcsin; *Corros. Sci.*, **2013**, *69*, 389-395.
27. M. Bobina; N. Vaszilcsin; C. Muntean; *Rev. Chim.-Bucharest*, **2013**, *64*, 83-88.
28. A. Samide; G. E. Iacobescu; B. Tutunaru; R. Grecu; C. Tigae; C. Spînu; *Coatings*, **2017**, *7*, 181.
29. A. Kokalj, C*orros. Sci.*, **2021** 196, 109939.